

Cell death-inducing DFF45-like effector C gene silencing alleviates pulmonary vascular remodeling in a type 2 diabetic rat model

Dong-xin Sui^{1,2}, Hui-min Zhou¹, Feng Wang¹, Ming Zhong¹, Wei Zhang¹, Yun Ti^{1*} 

¹The Key Laboratory of Cardiovascular Remodeling and Function Research, Chinese Ministry of Education and Chinese Ministry of Health, and The State and Shandong Province Joint Key Laboratory of Translational Cardiovascular Medicine, Department of Cardiology, Qilu Hospital of Shandong University, and ²Department of Respiration, the Second Hospital of Shandong University, Jinan, Shandong, China

Keywords

Cell death-inducing DFF45-like effector C, Diabetes, Pulmonary vascular remodeling

*Correspondence

Yun Ti

Tel.: +86-531-8216-9391

Fax: +86-531-8616-9356

E-mail address:

tiyunsdu@163.com

J Diabetes Investig 2018; 9: 741–752

doi: 10.1111/jdi.12768

ABSTRACT

Aims/Introduction: Cell death-inducing DFF45-like effector C (*CIDE*C) was proven to be closely associated with the development of insulin resistance and metabolic syndrome. We aimed to investigate whether *CIDE*C gene silencing could alleviate pulmonary vascular remodeling in a type 2 diabetes rat model.

Materials and Methods: We built a type 2 diabetes rat model. An adenovirus harboring *CIDE*C small interfering ribonucleic acid was then injected into the jugular vein to silence the *CIDE*C gene. After hematoxylin–eosin and Sirius red staining, we detected indexes of the pulmonary arterioles remodeling. Immunohistochemical staining of proliferating cell nuclear antigen was used to evaluate the pulmonary arterial smooth muscle cell proliferation. Apoptosis was evaluated by terminal deoxynucleotidyl transferase dUTP nick end labeling reaction and western blotting. The levels of signaling pathway proteins expression were measured by western blotting analyses.

Results: Histological analysis of the pulmonary artery showed that the thickness of the adventitia and medial layer increased notably in type 2 diabetes rats. Immunohistochemistry showed that more proliferating cell nuclear antigen-positive pulmonary arterial smooth muscle cells could be seen in type 2 diabetes rats; and after *CIDE*C gene silencing, proliferating cell nuclear antigen positive cells decreased accordingly. Cleaved caspase-3 and cleaved poly (adenosine diphosphate-ribose) polymerase measured by western blotting showed increased apoptosis with overexpressed *CIDE*C in diabetes. Terminal deoxynucleotidyl transferase dUTP nick end labeling reaction showed that the apoptosis mainly occurred in endothelial cells. Western blotting analysis showed *CIDE*C overexpression in rats with diabetes, and phosphorylated adenosine 5' monophosphate-activated protein kinase- α expression was significantly decreased. After *CIDE*C gene silencing, the expression of phosphorylated adenosine 5' monophosphate-activated protein kinase- α was upregulated.

Conclusions: The *CIDE*C/5' monophosphate-activated protein kinase signaling pathway could be a potential therapeutic candidate against pulmonary vascular diseases in type 2 diabetes patients.

INTRODUCTION

Pulmonary hypertension (PH) is a complex disease with significant morbidity and mortality. Pulmonary vascular remodeling,

including endothelial apoptosis and dysfunction, medial layer smooth muscle cell proliferation, adventitial fibroblast activation, differentiation and proliferation, and collagen synthesis, plays a key role in pulmonary hypertension^{1–3}. Recent studies suggested that the metabolic dysregulation might be an

Received 5 June 2017; revised 6 October 2017; accepted 23 October 2017

important factor contributing to the pulmonary vascular remodeling. Diabetes and metabolic syndrome were considered to be strongly associated with PH independent of coronary artery disease, congestive heart failure or smoking⁴. The procedures and mechanisms of pulmonary vascular remodeling associated with metabolic syndrome are complex, including endothelial dysfunction, medial smooth muscle cell proliferation, adventitial fibroblast activation and collagen synthesis^{5–7}. A number of inflammatory cells and cytokines, such as adipocytes, macrophages and adiponectin are involved in this pathophysiological process. Adenosine 5'-monophosphate activated protein kinase (AMPK), a key molecule in the regulation of energy metabolism, plays an important role in the study of diabetes and other metabolic diseases. Recent studies have shown that the activation of AMPK could inhibit the pulmonary arterial smooth muscle cell proliferation^{8–10}, and reduce collagen production in the lung and kidney^{11,12}.

The cell death-inducing DFF45-like effector (CIDE) family proteins could induce cell apoptosis. CIDE (known as Fsp27 in mice), which can be detected in many tissues, has been found to be closely associated with the development of metabolic diseases, such as obesity, diabetes and liver steatosis^{13–15}. Studies showed that CIDE could directly interact with the AMPK α 1 subunit and downregulate AMPK α through an ubiquitin/proteasome pathway¹⁶. Therefore, the overexpression of CIDE could significantly reduce AMPK activity¹⁷.

Thus, we hypothesized that type 2 diabetes and insulin resistance upregulated the protein expression of CIDE in lung tissue, which reduced the expression of AMPK, resulting in pulmonary vascular remodeling. *CIDE* gene silencing can contribute to decreasing pulmonary arterioles remodeling and pulmonary hypertension induced by diabetes. We established a type 2 diabetes Sprague–Dawley rat model, and used *CIDE* gene silencing to determine the relationships among the CIDE/AMPK signaling pathway, type 2 diabetes and pulmonary vascular remodeling.

EXPERIMENTAL GROUPS

A total of 40 male Sprague–Dawley rats were randomly assigned to the following four groups: normal control group (group C, 10 rats), type 2 diabetes group (group D, 10 rats), type 2 diabetes + *CIDE* small interfering ribonucleic acid adenovirus (*CIDE* gene silencing) group (group A, 10 rats) and type 2 diabetes + empty pAdxsi virus (vehicle) group (group V, 10 rats).

Animal model

Group C received normal chow, including 20% protein, 3% fat, 3% dietary fiber and 74% other components (carbohydrates, microelement, etc.). The type 2 diabetes group was fed a high-glucose and high-fat diet (34.5% fat, 17.5% protein and 48% carbohydrates). 4 weeks later, intraperitoneal glucose tolerance test and intraperitoneal insulin tolerance test were carried out again, and diabetes was induced by a single intraperitoneal

injection of streptozotocin (Sigma, St. Louis, MO, USA; 27.5 mg/kg i.p. in 0.1 mol/L citrate buffer, pH 4.5) to rats with insulin resistance. Group C received citrate buffer (i.p.) alone. 1 week after streptozotocin administration, fasting blood glucose (FBG) and fasting insulin (FINS) were measured, and the insulin sensitivity index (insulin sensitivity index = $\ln [FINS \times FBG]^{-1}$) was calculated. Rats with FBG \geq 11.1 mmol/L in two consecutive analyses and reduced insulin sensitivity were considered the diabetes rat model. After 12 weeks of diabetes, the type 2 diabetes group rats were randomized to receive *CIDE* small interfering ribonucleic acid for *CIDE* gene silencing or vehicle treatment. Animals were then injected in the jugular vein with 5×10^9 plaque-forming units of an adenovirus harboring *CIDE* small interfering ribonucleic acid to silence the *CIDE* gene or control empty pAdxsi virus (vehicle). After 4 weeks, bodyweight, FBG and FINS were measured again, and then all the rats were killed. All experimental procedures were carried out in accordance with animal protocols approved by the Shandong University Animal Care Committee.

Echocardiography test

According to recent studies, pulmonary artery acceleration time (PAAT) has been confirmed to be correlated with invasive pulmonary artery pressure, especially in mild-to-moderate pulmonary arterial hypertension¹⁸. Therefore, we calculated the PAAT by echocardiography to evaluate the mean pulmonary artery pressure. At the 21st week, pulsed-wave Doppler of pulmonary outflow was recorded in the parasternal view at the level of the aortic valve. PAAT was measured from the time of onset of systolic flow to peak pulmonary outflow velocity. The rats were killed after the echocardiography tests. The right ventricle (RV) tissue was cut along the edge of the ventricle and the interventricular septum. The RV and the left ventricle plus the interventricular septum were collected from each rat. They were weighed, and the mass ratio of the RV over the left ventricle plus the interventricular septum was used as an index for RV hypertrophy.

Histological analysis

The left lungs of each rat were removed, fixed in 4% paraformaldehyde for 24 h and then imbedded in paraffin. Tissue sections were cut 4 μ m in thickness. Pulmonary arterial smooth muscle cell proliferation was observed by hematoxylin–eosin (HE) staining, and the zone that the smooth muscle cells were distributed in was used to evaluate the area and thickness of the medial layer. The adventitial fibrosis was observed by evaluation of Sirius red staining. Green-, yellow- and red-stained collagen fibers were quantified as a measure of the area and thickness of the adventitia. Histological analysis of pulmonary vascular remodeling was carried out using light microscopy. One tissue section was chosen from each rat, and 5–10 pulmonary arterioles with diameters between 50–200 μ m were chosen randomly in each section. The pulmonary arteriole remodeling indexes were measured by

Table 1 | Baseline data

	Group C	Group D	Group V	Group A	<i>n</i>
Bodyweight (g)	168.14 ± 4.34	170 ± 3.55	169.71 ± 3.56	169.29 ± 3.50	7
FBG (mmol/L)	4.30 ± 0.18	4.84 ± 0.21	4.93 ± 0.39	4.27 ± 0.15	7–10
FINS (µg/dL)	3.61 ± 0.93	2.61 ± 0.35	2.61 ± 0.22	2.48 ± 0.40	6
ISI	−2.65 ± 0.21	−2.68 ± 0.18	−2.46 ± 0.13	−2.30 ± 0.13	6

Bodyweight, fasting blood glucose (FBG), fasting insulin and insulin sensitivity index (ISI) had no statistically significant difference among the four groups.

Image-Pro Plus 6.0 software (Media Cybernetics, Rockville, MD, USA). The medial layer thickness index = medial layer thickness / vessel wall thickness (HE, magnification: × 400), the medial layer area index = medial layer area/vessel wall area (HE, magnification: × 400), the adventitia thickness index = adventitia thickness / vessel wall thickness (Sirius red staining, magnification: × 200) and the adventitia area index = adventitia area / vessel wall area (Sirius red staining, magnification: × 200).

Immunohistochemistry

Paraffin embedded tissue sections were prepared as mentioned before. After blocking, sections were incubated with a mouse monoclonal antibody to proliferating cell nuclear antigen (PCNA; Abcam, Cambridge, UK). Sections were then incubated with secondary horseradish peroxidase labeled anti-rabbit immunoglobulin G polymer (PV-9001; Beijing Zhong Shan Golden Bridge Biotechnology Co. Ltd., Beijing, China). Lung specimens incubated with 0.01 mmol/L phosphate-buffered

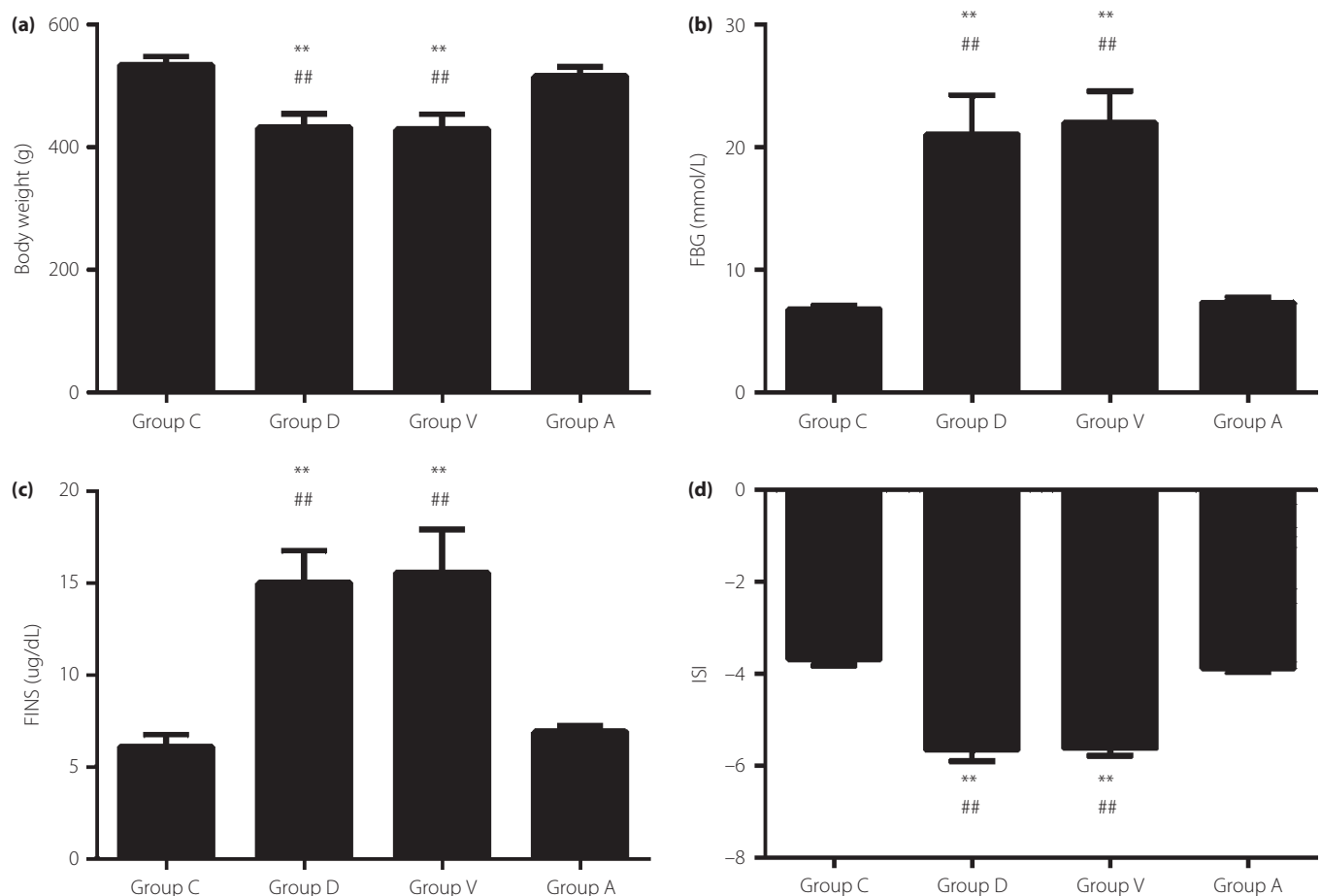


Figure 1 | Body weight, fasting blood glucose (FBG) and fasting insulin (FINS) of the four groups at the 21st week. (a) Bodyweights. (b) FBG. (c) FINS. (d). ISI (***P* < 0.01 vs group C; ##*P* < 0.01 vs group A).

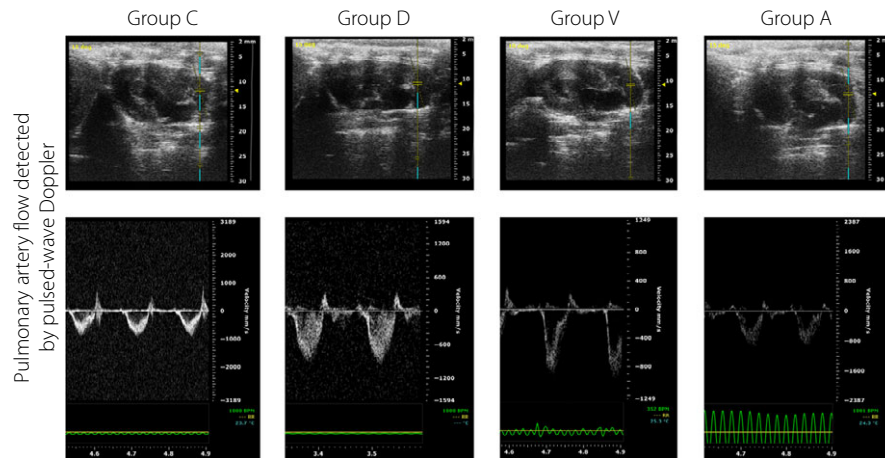


Figure 2 | Pulmonary artery flow detected by pulse-wave Doppler.

saline in place of the specific primary antibody served as negative controls. The nuclei stained brown or brown yellow can be determined as positive results. The percentage of the PCNA-positive cells in the total arterial medial layer smooth muscle cells, defined as the cell proliferation index, was used to evaluate the pulmonary arterial smooth muscle cell proliferation. The cell proliferation index (magnification: $\times 200$) in each group was statistically analyzed by Image-Pro Plus 6.0 image analysis software.

Analysis of apoptosis

As CIDEC was known to be a potent apoptotic inducer, we also evaluated apoptosis in pulmonary arterial endothelial cells and smooth muscle cells of the four groups. Apoptosis was evaluated by terminal deoxynucleotidyl transferase dUTP nick end labeling (TUNEL) reaction (FragEL™ DNA Fragmentation Detection Kit, Colorimetric-TdT Enzyme; EMD Millipore, Billerica, MA, USA). The nuclei stained brown could be determined as TUNEL-positive results. The percentage of the TUNEL-positive cells was defined as the cell apoptotic index (AI). The AI (magnification: $\times 400$) in each group was statistically analyzed by Image-Pro Plus 6.0 image analysis software. CIDEC (Abcam), cleaved caspase-3 (Cell Signaling Technology, Beverly, MA, USA) and cleaved poly (adenosine diphosphate-ribose) polymerase (PARP; Anti-Cleaved PARP Antibody; Boster Biological Technology, Wuhan, China) in lung tissue was measured by Western blotting subsequently to detecting the apoptosis.

Western blotting

After the rats were killed, the right lung tissue was divided into several 100-mg segments, and then was kept in the -80°C liquid nitrogen for protein analysis. The primary antibodies included a rabbit polyclonal CIDEC antibody (Abcam), a rabbit polyclonal AMPK α antibody (Cell Signaling Technology), a rabbit polyclonal phosphorylated AMPK α antibody (Cell

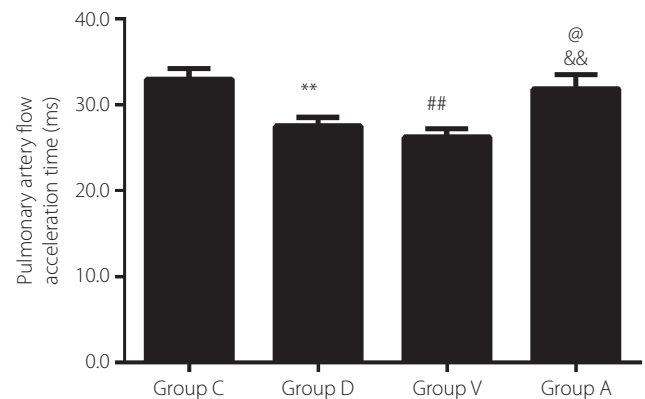


Figure 3 | Pulmonary artery acceleration time measured by pulse-wave Doppler in each group (** $P < 0.01$, ## $P < 0.01$ vs group C, @ $P < 0.05$ vs group D, && $P < 0.01$ vs group V).

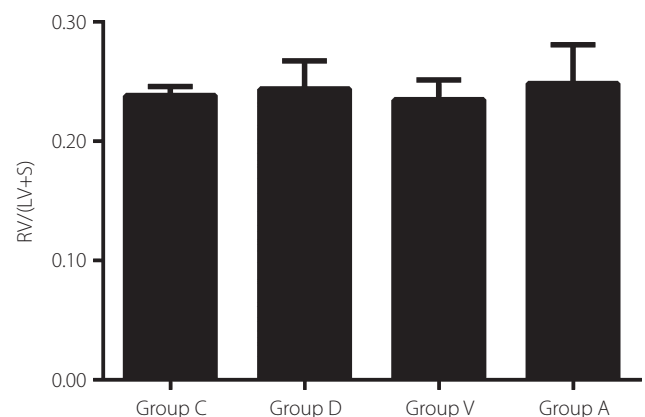


Figure 4 | The indexes of right ventricular hypertrophy (RVH) of the four groups ($P > 0.05$). LV + S, left ventricle plus the interventricular septum.

Signaling Technology) and a mouse monoclonal β -actin antibody (Abcam). The secondary antibodies included a goat anti-rabbit immunoglobulin G/horseradish peroxidase (ZDR-5306;

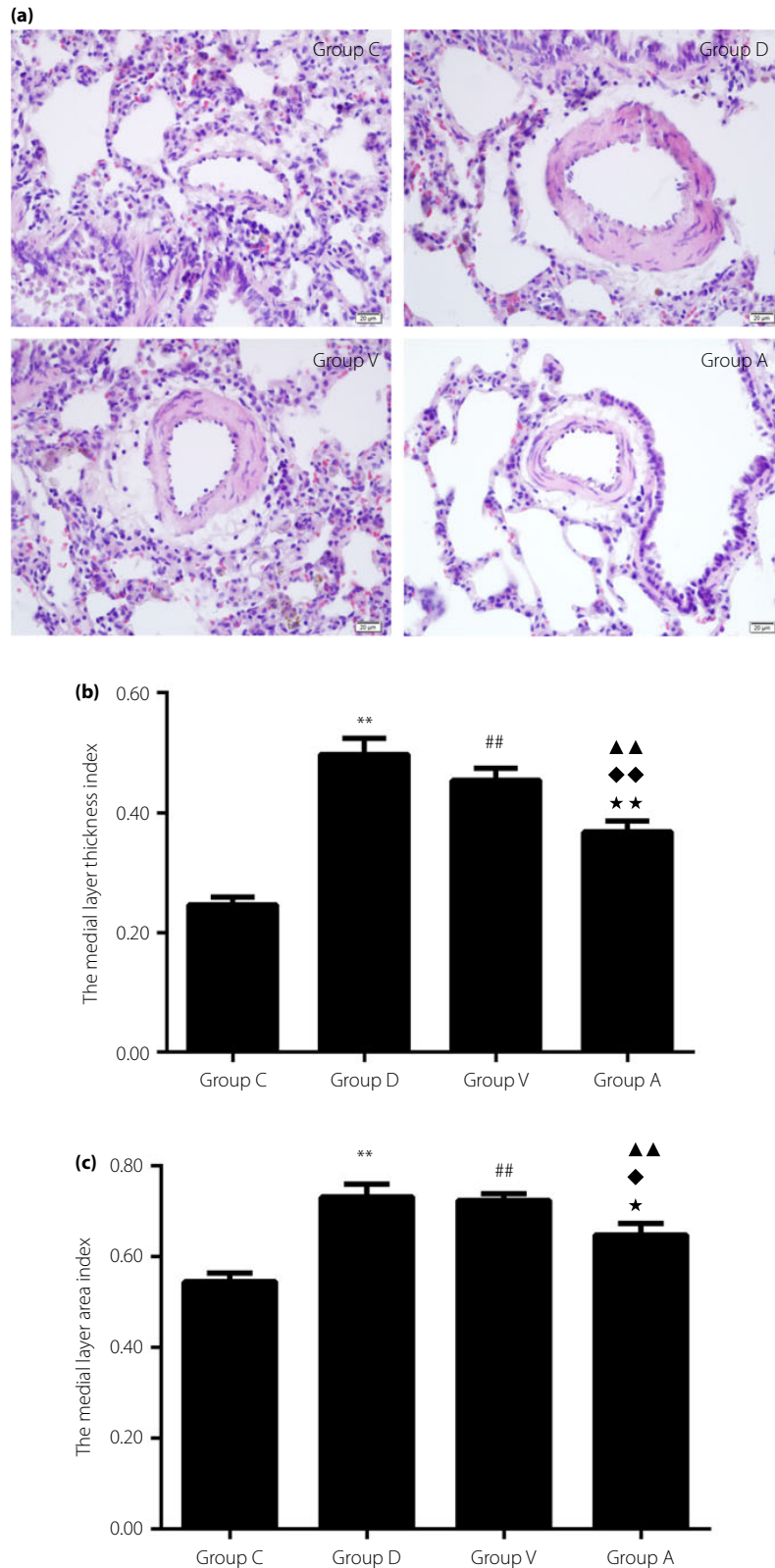


Figure 5 | (a) Pulmonary arterial smooth muscle cell proliferation observed by hematoxylin–eosin staining. (b) The medial layer thickness index (** $P < 0.01$, ## $P < 0.01$ vs group C, ▲▲ $P < 0.01$ vs group C, ◆◆ $P < 0.01$ vs group D, ★★ $P < 0.01$ vs group V). (c) The medial layer area index (** $P < 0.01$, ## $P < 0.01$ vs group C), ▲▲ $P < 0.01$ vs group C, ◆ $P < 0.05$ vs group D, ★ $P < 0.05$ vs group V).

Beijing Zhong Shan Golden Bridge Biotechnology Co. Ltd.) and a goat anti-mouse immunoglobulin G/horseradish peroxidase (ZDR-5307; Beijing Zhong Shan Golden Bridge Biotechnology Co. Ltd.). The relative optical density of electrophoretic bands was quantitatively calculated by Image-Pro Plus 6.0 image analysis software.

Statistical analysis

All data are expressed as the mean \pm standard error. SPSS Statistics 17.0 (SPSS Inc., Chicago, IL, USA) was used to carry out all the calculations. ANOVA followed by a Tukey–Kramer

test was used for statistical analyses of differences between groups. A level of $P < 0.05$ was considered statistically significant.

RESULTS

Bodyweight, FBG and FINS of the four groups

As expected, at the 21st week, bodyweights and insulin sensitivity indexes were significantly lower in group D and group V than in group C and group A, and FBGs and FINSs were significantly higher in group D and group V than in group C and group A (Table 1; Figure 1).

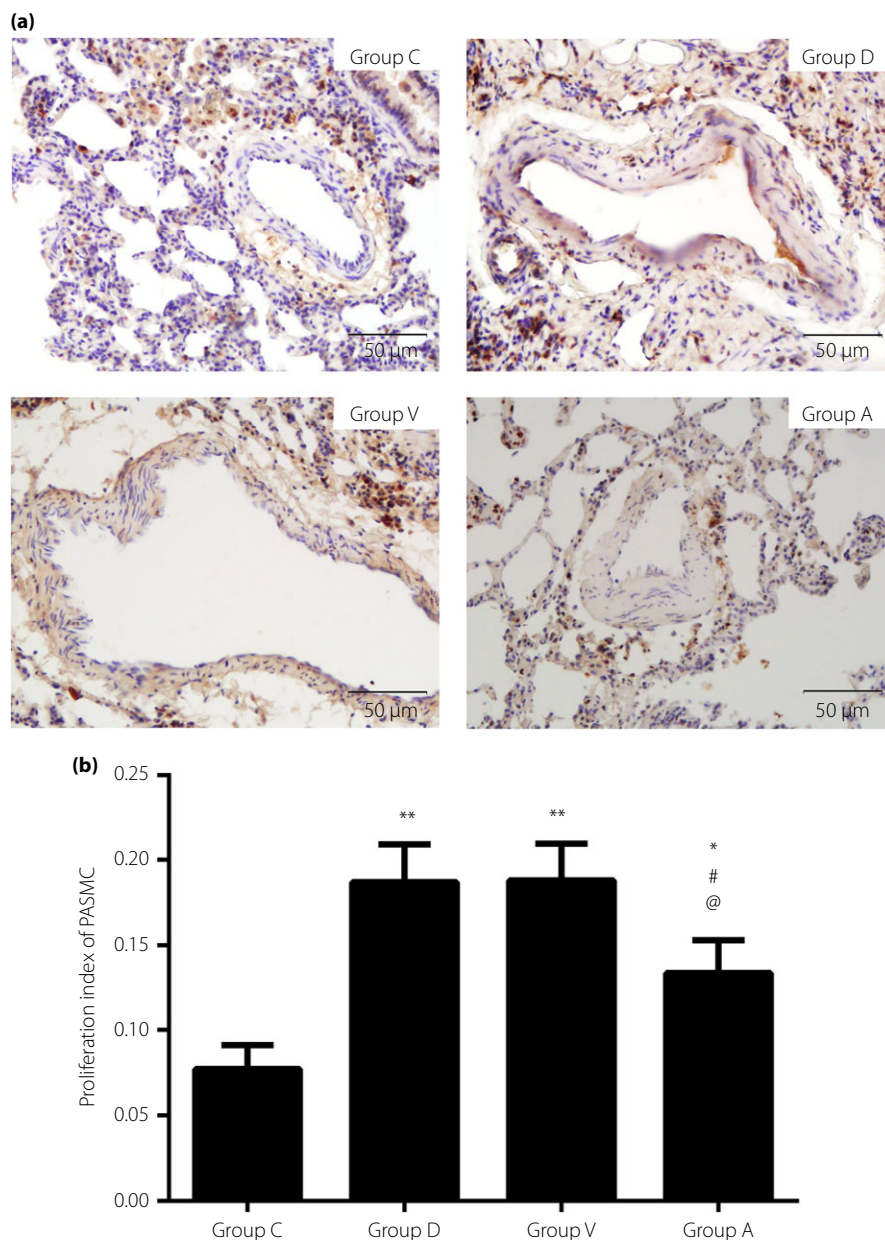


Figure 6 | (a) Pulmonary arterial smooth muscle cell (PASMC) proliferation evaluated by immunohistochemical staining of proliferating cell nuclear antigen. (b) The cell proliferation indexes (** $P < 0.01$, * $P < 0.05$ vs Group C, # $P < 0.05$ vs group D, @ $P < 0.05$ vs group V).

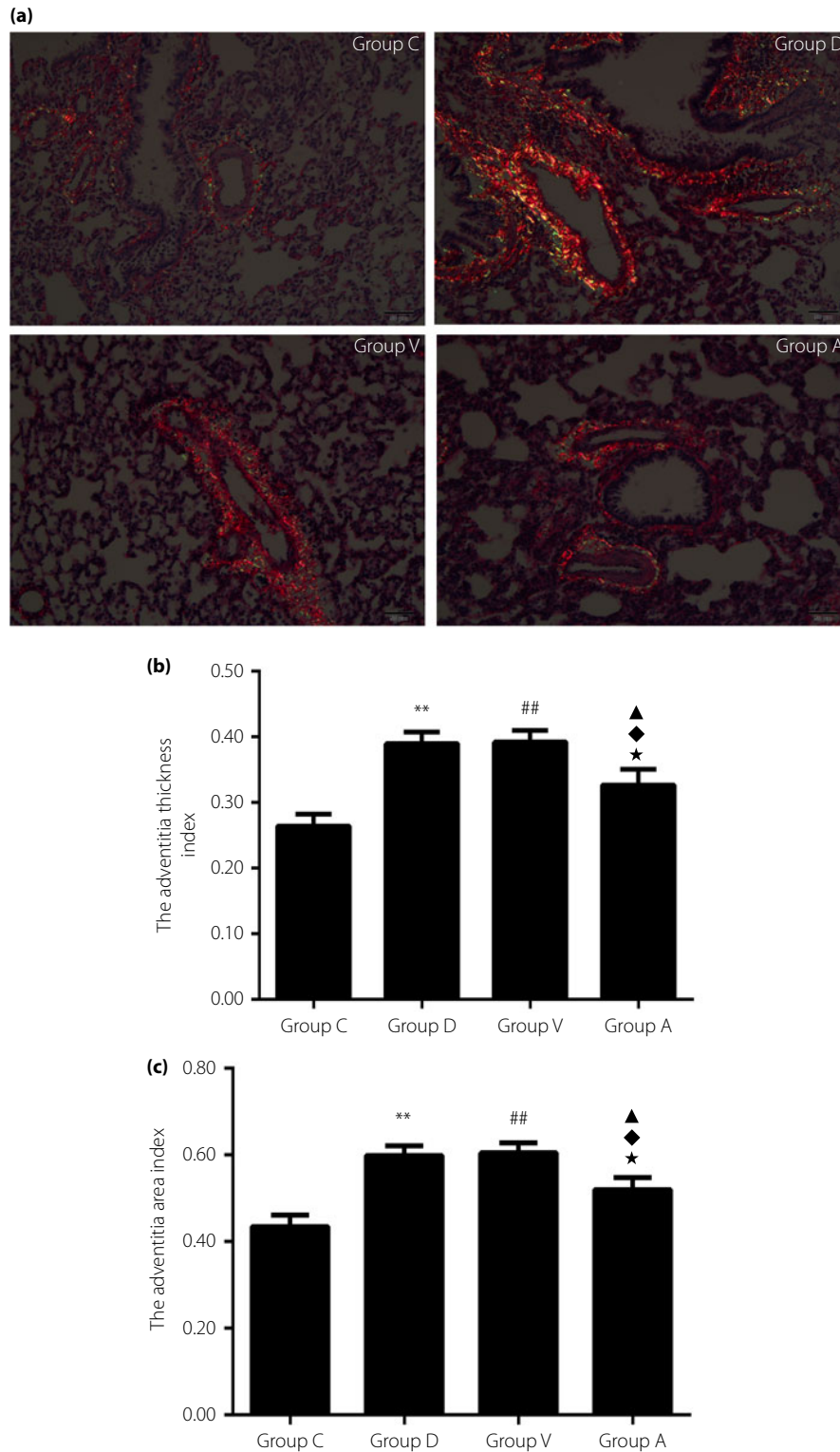


Figure 7 | (a) The adventitial fibrosis observed by Sirius red staining. (b) The adventitia thickness index (** $P < 0.01$, ## $P < 0.01$ vs group C, ▲ $P < 0.05$ vs group C, ♦ $P < 0.05$ vs group D, ★ $P < 0.05$ vs group V). (c) The adventitia area index (** $P < 0.01$, ## $P < 0.01$ vs group C, ▲ $P < 0.05$ vs group C, ♦ $P < 0.05$ vs group D, ★ $P < 0.05$ vs group V).

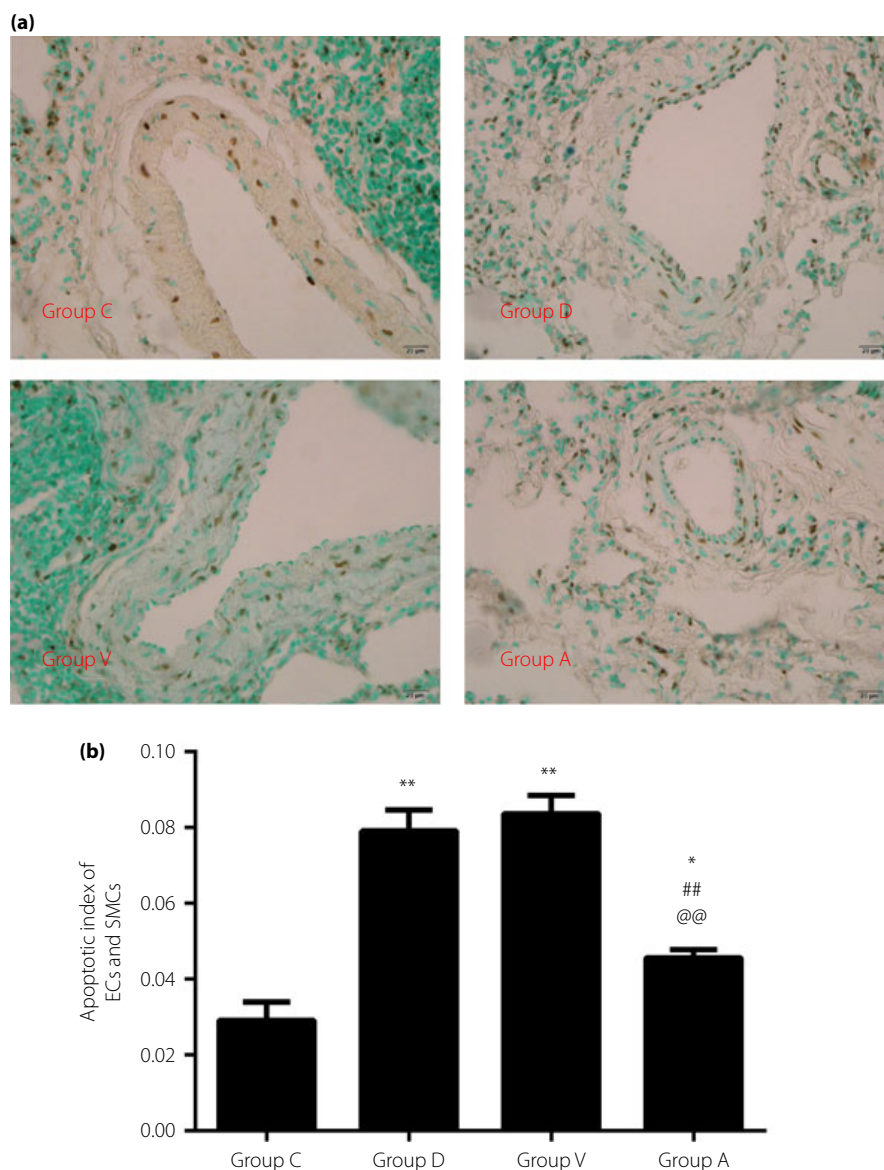


Figure 8 | (a) The apoptosis of the pulmonary arterial endothelial cells (ECs) and smooth muscle cells (SMCs) detected by terminal deoxynucleotidyl transferase dUTP nick end labeling reaction. (b) The apoptotic indexes (** $P < 0.01$, * $P < 0.05$ vs group C, ## $P < 0.01$ vs group D, @@ $P < 0.01$ vs group V).

Effects of diabetes and CIDEc gene silencing on PAAT and RV hypertrophy

At the 21st week, pulsed-wave Doppler of pulmonary outflow was recorded to measure the PAAT (Figure 2). PAAT was significantly shortened in group D and group V compared with group C. After *CIDEc* gene silencing, PAAT was lengthened correspondingly (Figure 3). The index of RV hypertrophy had no statistically significant difference among the four groups (Figure 4).

Histological analysis of pulmonary vascular remodeling

Pulmonary arterial smooth muscle cell proliferation was observed by HE staining. In group D and group V rats, the

pulmonary arterioles medial layer had thickened, as a result of the smooth muscle cell proliferation. However, in group A rats, the smooth muscle cell proliferation and the medial layer thickening in the pulmonary arterioles were reduced (Figure 5a). The medial layer thickness index of group D and group V were significantly increased compared with those of group C (group D vs group C: 0.4972 ± 0.0265 vs 0.2461 ± 0.0130 , $P < 0.01$; group V vs group C: 0.4537 ± 0.0204 vs 0.2461 ± 0.0130 , $P < 0.01$). After *CIDEc* gene silencing, the medial layer thickness indexes were significantly decreased compared with those of group D and group V (Figure 5b). Similar results were obtained when compared with the medial layer area index among the four groups (Figure 5c). Immunohistochemical

staining of PCNA was used to evaluate the pulmonary arterial smooth muscle cell proliferation. More PCNA-positive pulmonary arterial medial layer smooth muscle cells could be seen in group D and group V, and after *CIDEC* gene silencing, PCNA-positive cells decreased accordingly (Figure 6a). The cell proliferation indexes were significantly higher in group D and group V (group D vs group C: 0.187 ± 0.022 vs 0.077 ± 0.014 , $P < 0.01$; group V vs group C: 0.188 ± 0.021 vs 0.077 ± 0.014 , $P < 0.01$), and after *CIDEC* gene silencing, the proliferation index became lower accordingly (group A vs group C: 0.134 ± 0.019 vs 0.077 ± 0.014 , $P < 0.05$; group A vs group D: 0.134 ± 0.019 vs 0.187 ± 0.022 , $P < 0.05$; group A vs group V: 0.134 ± 0.019 vs 0.188 ± 0.021 , $P < 0.05$; Figure 6b).

The adventitial fibrosis was observed and evaluated by Sirius red staining. Green-, yellow- and red-stained collagen fibers were quantified as a measure of the area and thickness of the adventitia. In group D and group V rats, the pulmonary arterioles adventitia had thickened as a result of the collagen deposition. After *CIDEC* gene silencing, the collagen deposition and the adventitia thickening in the pulmonary arterioles were reduced (Figure 7a). The adventitia thickness index of group D and group V were significantly increased compared with those of group C (group D vs group C: 0.3899 ± 0.0176 vs 0.2642 ± 0.0186 , $P < 0.01$; group V vs group C: 0.3921 ± 0.0175 vs 0.2642 ± 0.0186 , $P < 0.01$). After *CIDEC* gene silencing, the adventitia thickness indexes were significantly decreased compared with those of group D and group V (Figure 7b). Similar results were obtained when compared with the adventitia area index among the four groups (Figure 7c).

Analysis of apoptosis

TUNEL was applied to detect the apoptosis of the pulmonary arterial endothelial cells and smooth muscle cells. More TUNEL-positive cells could be detected in group D and group V. After *CIDEC* gene silencing, TUNEL-positive cells decreased accordingly, and as observed, the differences in apoptosis mainly occurred in endothelial cells (Figure 8a). The AIs were significantly higher in group D and group V (group D vs group C: 0.0791 ± 0.0056 vs 0.0292 ± 0.0047 , $P < 0.01$; group V vs group C: 0.0837 ± 0.0047 vs 0.0292 ± 0.0047 , $P < 0.01$), and after *CIDEC* gene silencing, AI became lower accordingly (group A vs group C: 0.0530 ± 0.008 vs 0.0292 ± 0.0047 , $P < 0.05$; group A vs group D: 0.0530 ± 0.008 vs 0.0791 ± 0.0056 , $P < 0.01$; group A vs group V: 0.0530 ± 0.008 vs 0.0837 ± 0.0047 , $P < 0.01$; Figure 8b). Cleaved caspase-3 and cleaved PARP in lung tissue of rats were measured by western blotting (Figure 9a). Both cleaved caspase-3 and cleaved PARP were significantly overexpressed in group D and group V compared with group C. After *CIDEC* gene silencing, the expression of cleaved caspase-3 and cleaved PARP were relatively downregulated (Figure 9b,c).

Expression of signaling pathway proteins in lung tissue

Protein expression of *CIDEC*, AMPK α and phosphorylated AMPK α in lung tissue of rats were measured by western

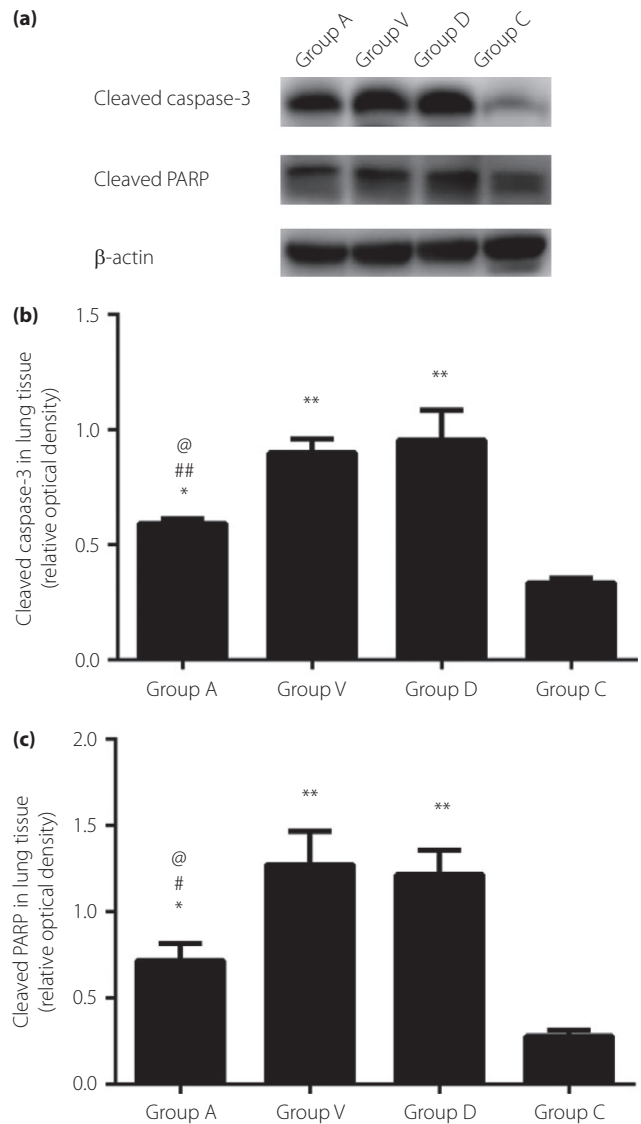


Figure 9 | (a) Cleaved caspase-3 and cleaved poly (adenosine diphosphate-ribose) polymerase (PARP) in lung tissue measured by western blotting. (b) Cleaved caspase-3 (** $P < 0.01$, * $P < 0.05$ vs group C, ## $P < 0.01$ vs group D, @ $P < 0.05$ vs group V). (c) Cleaved PARP (** $P < 0.01$, * $P < 0.05$ vs group C, # $P < 0.05$ vs group D, @ $P < 0.05$ vs group V).

blotting (Figure 10a). *CIDEC* was significantly overexpressed in group D and group V compared with group C. After *CIDEC* gene silencing, the expression of *CIDEC* was significantly downregulated (Figure 10b). The expression of phosphorylated AMPK α was significantly decreased in group D and group V compared with group C. After *CIDEC* gene silencing, the expression of phosphorylated AMPK α in group A was significantly increased, and had no statistically significant difference compared with group C (Figure 10c). The expression of AMPK α had no statistically significant difference among the four groups ($P > 0.05$; Figure 10d).

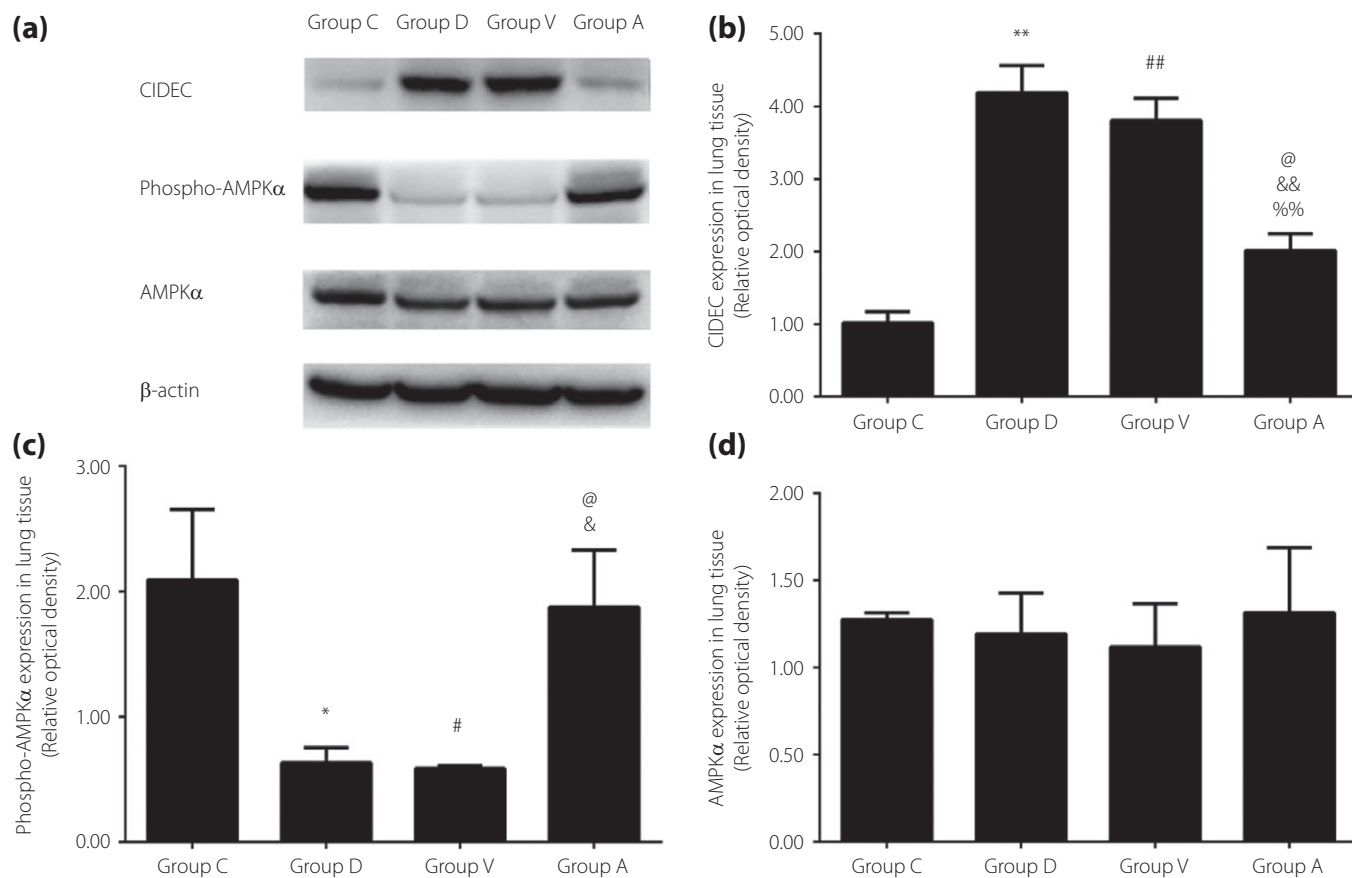


Figure 10 | (a) Protein expression of cell death-inducing DFF45-like effector C (CIDEc), adenosine 5' monophosphate-activated protein kinase- α (AMPK α) and phosphorylated AMPK α measured by western blotting. (b) CIDEc (** $P < 0.01$, ## $P < 0.01$, @ $P < 0.05$ vs group C, && $P < 0.01$ vs group D, % $P < 0.01$ vs group V). (c) Phosphorylated AMPK α (* $P < 0.05$, # $P < 0.05$ vs group C, @ $P < 0.05$ vs group D, & $P < 0.05$ vs group V). (d) AMPK α ($P > 0.05$).

DISCUSSION

The salient finding of the present study was that the CIDEc/AMPK signaling pathway plays a major role in the pulmonary vascular remodeling in a type 2 diabetes rat model. More importantly, silencing of *CIDEc* partially reversed diabetic pulmonary vascular remodeling. Thus, the CIDEc/AMPK signaling pathway could be a potential therapeutic candidate against pulmonary vascular diseases in type 2 diabetes.

We established a type 2 diabetes Sprague–Dawley rat model to investigate the relationships among the CIDEc/AMPK signaling pathway, type 2 diabetes and the pulmonary vascular remodeling. The *CIDEc* gene was silenced in order to study the effects of CIDEc. In the present study, the results showed that diabetes induced mildly elevated mean pulmonary artery pressure, and this process was partially reversed after the *CIDEc* gene silencing. The RV hypertrophy index of the four groups showed that diabetes had not induced notable RV hypertrophy yet. We detected the pulmonary arterioles remodeling by histological analysis. The pulmonary arterioles medial layer and the adventitia had thickened with diabetes as a result

of the smooth muscle cell proliferation and the collagen deposition. Cleaved caspase-3 and cleaved PARP in lung tissue measured by western blotting showed increased apoptosis with overexpressed CIDEc in diabetes. TUNEL reaction showed that the differences in apoptosis mainly occurred in endothelial cells. Therefore, the present study showed that diabetes could cause pulmonary vascular remodeling at least by endothelial apoptosis, medial layer smooth muscle cell proliferation, adventitial fibroblast activation and collagen synthesis. These findings were consistent with the reported characteristics of pulmonary vascular remodeling^{19,20}. As observed in the present study, silencing of *CIDEc* reversed the pathological pulmonary arterioles remodeling. Protein expression of CIDEc has been detected by western blotting in the lung tissue of each group. In rats with diabetes, CIDEc was significantly overexpressed, which induced the downregulation of the expression of phosphorylated AMPK α . After *CIDEc* gene silencing, the expression of phosphorylated AMPK α was significantly increased.

Pulmonary vascular remodeling plays a key role in pulmonary hypertension. Many systemic diseases, including chronic

obstructive pulmonary disease, chronic pulmonary thromboembolism and connective tissue disease, were considered to contribute to pulmonary vascular remodeling and PH^{21–24}. Recent animal and human studies have highlighted that metabolic dysregulation and chronic inflammation were linked to the development of pulmonary vascular remodeling. As the most common and important metabolic disorder, diabetes was considered to be strongly associated with PH. In diabetes, vascular remodeling extends to capillaries, microvascular beds and arteries of different caliber. As an important part of the circulatory system, pulmonary vessels are also affected by diabetes, and more attention has been paid to the mechanisms of pulmonary vascular remodeling associated with diabetes^{6,7,25,26}. The present study showed that diabetes could induce pulmonary arterioles remodeling and have mild hemodynamic effects on pulmonary circulation. Numerous molecules have been proven to be associated with diabetic pulmonary vascular remodeling, including nicotinamide adenine dinucleotide phosphate oxidase, peroxisome proliferator-activated receptor gamma, Caveolin-1 and so on⁶. AMPK is a key molecule in the regulation of biological energy metabolism. It plays an important role in regulating cell growth and proliferation, establishing and stabilizing cell polarity, and regulating physiological rhythm. The effect of AMPK on pulmonary hypertension induced by chronic hypoxia has been reported⁹. The role of AMPK in diabetic pulmonary vascular remodeling is yet to be confirmed. CIDEc (known as Fsp27 in mice) was proven to be closely associated with the development of insulin resistance and metabolic syndrome^{13–15}. Studies showed that CIDEc and CIDEa could directly interact with the AMPK α 1 subunit and downregulate AMPK α through an ubiquitin/proteasome pathway, and CIDEc could also influence the activity of AMPK by phosphorylation^{16,17,27}. Therefore the overexpression of AMPK could significantly reduce AMPK activity¹⁷. The present research confirmed that diabetes and insulin resistance upregulated the protein expression of CIDEc in lung tissue, which inhibited the AMPK signaling pathway and induced pulmonary arterioles remodeling, and the protective effects with CIDEc silencing suggested a potential role in treating diabetic pulmonary vascular diseases.

ACKNOWLEDGMENTS

This work was supported by research grants from the National Natural Science Foundation of China (81300168, 81471036, 81470560, 30971215, 81570400, 81600633, 81670411, 81270352, 81270287, 81100605, 91439201, 81530014 and 81320108004), the National Basic Research Program of China (973 Program, Grant No. 2013CB530703), Key Research and Development Program of Shandong Province (2015GSF118062), the Natural Science Foundation of Shandong Province (BS2011YY024, ZR2014HQ037), the Specialized Research Fund for the Doctoral Program of Higher Education (SRFDP 20130131120065), and Program of Introducing Talents of Discipline to Universities (B07035).

DISCLOSURE

The authors declare no conflict of interest.

REFERENCES

- Lai YC, Potoka KC, Champion HC, *et al.* Pulmonary arterial hypertension: the clinical syndrome. *Circ Res* 2014; 115: 115–130.
- Paulin R, Michelakis ED. The metabolic theory of pulmonary arterial hypertension. *Circ Res* 2014; 115: 148–164.
- Rabinovitch M, Guignabert C, Humbert M, *et al.* Inflammation and immunity in the pathogenesis of pulmonary arterial hypertension. *Circ Res* 2014; 115: 165–175.
- Movahed MR, Hashemzadeh M, Jamal MM. The prevalence of pulmonary embolism and pulmonary hypertension in patients with type II diabetes mellitus. *Chest* 2005; 128: 3568–3571.
- Moral-Sanz J, Lopez-Lopez JG, Menendez C, *et al.* Different patterns of pulmonary vascular disease induced by type 1 diabetes and moderate hypoxia in rats. *Exp Physiol* 2012; 97: 676–686.
- Mathew R. Pulmonary hypertension and metabolic syndrome: possible connection, PPARgamma and Caveolin-1. *World J Cardiol* 2014; 6: 692–705.
- Moral-Sanz J, Moreno L, Cogolludo A, *et al.* Pulmonary vascular function in insulin resistance and diabetes. *Curr Vasc Pharmacol* 2014; 12: 473–482.
- Ibe JC, Zhou Q, Chen T, *et al.* Adenosine monophosphate-activated protein kinase is required for pulmonary artery smooth muscle cell survival and the development of hypoxic pulmonary hypertension. *Am J Respir Cell Mol Biol* 2013; 49: 609–618.
- Huang X, Fan R, Lu Y, *et al.* Regulatory effect of AMP-activated protein kinase on pulmonary hypertension induced by chronic hypoxia in rats: in vivo and in vitro studies. *Mol Biol Rep* 2014; 41: 4031–4041.
- Wu Y, Liu L, Zhang Y, *et al.* Activation of AMPK inhibits pulmonary arterial smooth muscle cells proliferation. *Exp Lung Res* 2014; 40: 251–258.
- Park CS, Bang BR, Kwon HS, *et al.* Metformin reduces airway inflammation and remodeling via activation of AMP-activated protein kinase. *Biochem Pharmacol* 2012; 84: 1660–1670.
- Lu J, Shi J, Li M, *et al.* Activation of AMPK by metformin inhibits TGF-beta-induced collagen production in mouse renal fibroblasts. *Life Sci* 2015; 127: 59–65.
- Moreno-Navarrete JM, Ortega F, Serrano M, *et al.* CIDEc/FSP27 and PLIN1 gene expression run in parallel to mitochondrial genes in human adipose tissue, both increasing after weight loss. *Int J Obes (Lond)* 2014; 38: 865–872.
- Reynolds TH, Banerjee S, Sharma VM, *et al.* Effects of a high fat diet and voluntary wheel running exercise on cidea and

- cidec expression in liver and adipose tissue of mice. *PLoS ONE* 2015; 10: e0130259.
15. Shamsi BH, Ma C, Naqvi S, *et al.* Effects of pioglitazone mediated activation of PPAR-gamma on CIDEc and obesity related changes in mice. *PLoS ONE* 2014; 9: e106992.
 16. Xu Y, Gu Y, Liu G, *et al.* Cidec promotes the differentiation of human adipocytes by degradation of AMPKalpha through ubiquitin-proteasome pathway. *Biochim Biophys Acta* 2015; 1850: 2552–2562.
 17. Wang ZQ, Yu Y, Zhang XH, *et al.* Human adenovirus 36 decreases fatty acid oxidation and increases de novo lipogenesis in primary cultured human skeletal muscle cells by promoting Cidec/FSP27 expression. *Int J Obes (Lond)* 2010; 34: 1355–1364.
 18. Koskenvuo JW, Mirsky R, Zhang Y, *et al.* A comparison of echocardiography to invasive measurement in the evaluation of pulmonary arterial hypertension in a rat model. *Int J Cardiovasc Imaging* 2010; 26: 509–518.
 19. Sakao S, Tatsumi K, Voelkel NF. Endothelial cells and pulmonary arterial hypertension: apoptosis, proliferation, interaction and transdifferentiation. *Respir Res* 2009; 10: 95.
 20. Yamaji-Kegan K, Takimoto E, Zhang A, *et al.* Hypoxia-induced mitogenic factor (FIZZ1/RELMalpha) induces endothelial cell apoptosis and subsequent interleukin-4-dependent pulmonary hypertension. *Am J Physiol Lung Cell Mol Physiol* 2014; 306: L1090–L1103.
 21. Condliffe R, Howard LS. Connective tissue disease-associated pulmonary arterial hypertension. *F1000Prime Rep* 2015; 7: 06.
 22. Galie N, Humbert M, Vachiery JL, *et al.* 2015 ESC/ERS guidelines for the diagnosis and treatment of pulmonary hypertension: the joint task force for the diagnosis and treatment of pulmonary hypertension of the European Society of Cardiology (ESC) and the European Respiratory Society (ERS) Endorsed by: Association for European Paediatric and Congenital Cardiology (AEPC), International Society for Heart and Lung Transplantation (ISHLT). *Eur Heart J* 2015; 37: 67–119.
 23. Klok FA, Mos I, van Kralingen K, *et al.* Chronic pulmonary embolism and pulmonary hypertension. *Semin Respir Crit Care Med* 2012; 33: 199–204.
 24. Sakao S, Voelkel NF, Tatsumi K. The vascular bed in COPD: pulmonary hypertension and pulmonary vascular alterations. *Eur Respir Rev* 2014; 23: 350–355.
 25. Pugh ME, Hemnes AR. Metabolic and hormonal derangements in pulmonary hypertension: from mouse to man. *Int J Clin Pract Suppl* 2010; 168: 5–13.
 26. Robbins IM, Newman JH, Johnson RF, *et al.* Association of the metabolic syndrome with pulmonary venous hypertension. *Chest* 2009; 136: 31–36.
 27. Qi J, Gong J, Zhao T, *et al.* Downregulation of AMP-activated protein kinase by Cidea-mediated ubiquitination and degradation in brown adipose tissue. *EMBO J* 2008; 27: 1537–1548.